

This article was downloaded by:

On: 23 January 2011

Access details: *Access Details: Free Access*

Publisher *Taylor & Francis*

Informa Ltd Registered in England and Wales Registered Number: 1072954 Registered office: Mortimer House, 37-41 Mortimer Street, London W1T 3JH, UK



Journal of Coordination Chemistry

Publication details, including instructions for authors and subscription information:

<http://www.informaworld.com/smpp/title~content=t713455674>

Syntheses, crystal structures, and fluorescence properties of two isomorphic binuclear compounds incorporating N-acetyl-N-phenylglycinate with N-donor co-ligands

Ai-Yun Fu^a; Ya-Pan Wu^b; Fu-Ming Wang^a; Yong-Ling Sun^a

^a Materials Chemistry Research Center, Dezhou University, Dezhou 253023, Shandong, P.R. China ^b

Department of Chemistry and Chemical Engineering, Shaanxi Key Laboratory of Chemical Reaction Engineering, Yan'an University, Yan'an, Shaanxi 716000, P.R. China

First published on: 04 October 2010

To cite this Article Fu, Ai-Yun , Wu, Ya-Pan , Wang, Fu-Ming and Sun, Yong-Ling(2010) 'Syntheses, crystal structures, and fluorescence properties of two isomorphic binuclear compounds incorporating N-acetyl-N-phenylglycinate with N-donor co-ligands', *Journal of Coordination Chemistry*, 63: 21, 3724 – 3733, First published on: 04 October 2010 (iFirst)

To link to this Article: DOI: 10.1080/00958972.2010.521551

URL: <http://dx.doi.org/10.1080/00958972.2010.521551>

PLEASE SCROLL DOWN FOR ARTICLE

Full terms and conditions of use: <http://www.informaworld.com/terms-and-conditions-of-access.pdf>

This article may be used for research, teaching and private study purposes. Any substantial or systematic reproduction, re-distribution, re-selling, loan or sub-licensing, systematic supply or distribution in any form to anyone is expressly forbidden.

The publisher does not give any warranty express or implied or make any representation that the contents will be complete or accurate or up to date. The accuracy of any instructions, formulae and drug doses should be independently verified with primary sources. The publisher shall not be liable for any loss, actions, claims, proceedings, demand or costs or damages whatsoever or howsoever caused arising directly or indirectly in connection with or arising out of the use of this material.

Syntheses, crystal structures, and fluorescence properties of two isomorphous binuclear compounds incorporating N-acetyl-N-phenylglycinate with N-donor co-ligands

AI-YUN FU*[†], YA-PAN WU[‡], FU-MING WANG[†] and YONG-LING SUN[†]

[†]Materials Chemistry Research Center, Dezhou University, Dezhou 253023, Shandong, P.R. China

[‡]Department of Chemistry and Chemical Engineering, Shaanxi Key Laboratory of Chemical Reaction Engineering, Yan'an University, Yan'an, Shaanxi 716000, P.R. China

(Received 17 December 2009; in final form 2 August 2010)

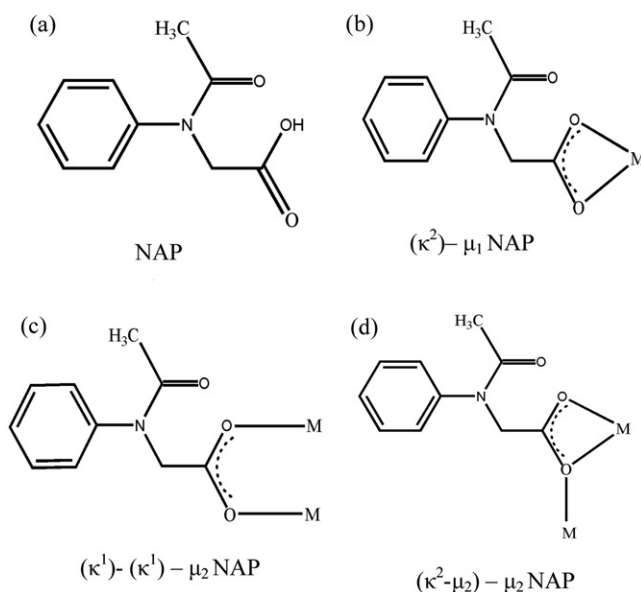
In this study, two new isomorphous binuclear compounds, $[\text{Ln}(\mu\text{-NAP})_4(\text{NAP})_2(\text{phen})_2] \cdot \text{H}_2\text{O}$ (**1**) and (**2**) (Ln = Eu, Tb, NAP = N-acetyl-N-phenylglycinate; phen = 1,10-phenanthroline), have been synthesized and characterized by infrared spectroscopy, elemental analysis, and X-ray crystallography. These compounds crystallize in a triclinic form with space group $P\bar{1}$ with $a = 11.7519(11)$, $b = 13.4293(12)$, $c = 14.0686(13)$ Å, $V = 1992.7(3)$ Å³, and $Z = 1$. Single-crystal X-ray structural analysis reveals that **1** is binuclear, assembled into a 3-D supramolecular network with self-complementary double hydrogen-bonding interactions and aromatic π - π interactions. Fluorescence properties of **1** and **2** are also discussed.

Keywords: Ln-based compounds; Crystal structure; Fluorescent properties; Thermal stability

1. Introduction

Design and synthesis of rare-earth organic-inorganic hybrid materials have provoked extensive interest in supramolecular chemistry and crystal engineering, although the flexibility of the coordination sphere of lanthanide ions makes design difficult compared with the predictability of the coordination geometry of the transition metals [1–3]. The coordination ambivalence, coupled with the tendency of lanthanides to adopt high coordination numbers and the rigidity of the organic ligands employed, makes f-block metals attractive for structures dictated by the different size of the lanthanide ions, resulting in interesting molecular topologies and crystal packing motifs [4–11]. These materials take advantage of the best properties of organic and inorganic components for potential applications as functional materials with optical, magnetic, catalytic, and electrical conductivity properties [12]. Consequently, a number of investigations on lanthanide coordination polymers have been published recently [13, 14].

*Corresponding author. Email: fuaiyun666@yahoo.com.cn

Scheme 1. Scheme for NAP and coordination modes in **1** and **2**.

Carboxylate ligands play an important role in constructing metal organic frameworks (MOFs) based on lanthanides, adopting diverse binding modes such as terminal monodentate, chelating to one metal center, bridging bidentate in *syn-syn*, *syn-anti*, or *anti-anti* configuration to two metal centers, and also supramolecular contacts such as hydrogen bonding, $\pi-\pi$ interactions, etc. [15]. The N-substituent N-acetyl-N-phenylglycinate (NAP) (see scheme 1a) is a very important carboxylate in coordination chemistry. NAP possessed one hydroxyl, one carboxylate, and a phenyl ring, which could provide network structures *via* dative bonds and also noncovalent contacts, such as hydrogen bonding and aromatic stacking, potentially providing various coordination modes to form both discrete and polymeric metal compounds under appropriate conditions. Rare-earth N-protected amino acids show novel networks and properties [16, 17]. However, metal-organic coordination polymers built from N-substituted amino acids attract less attention than carboxylate-containing ones. We were inspired to add auxiliary co-ligands to the reaction mixture to construct lanthanide coordination polymers. Herein, two isomorphous binuclear compounds, $[\text{Eu}(\mu\text{-NAP})_4(\text{NAP})_2(\text{phen})_2] \cdot \text{H}_2\text{O}$ (**1**) and $[\text{Tb}(\mu\text{-NAP})_4(\text{NAP})_2(\text{phen})_2] \cdot \text{H}_2\text{O}$ (**2**), were synthesized and characterized by elemental analyses, infrared (IR) spectroscopy, fluorescent measurements, and single-crystal X-ray diffraction analysis.

2. Experimental

2.1. Materials and methods

All chemicals were of analytical reagent grade and used as received. Fourier transform infrared spectroscopy (FT-IR) spectra were recorded from KBr pellets from 4000 to 400 cm^{-1} on a Bruker EQUINOX-55 spectrometer. Fluorescence spectra were

performed on a Hitachi F-4500 fluorescence spectrophotometer at room temperature. Elemental analysis was determined with an Elementar Vario EL III elemental analyzer. Thermal analyses were performed on a NETZSCH STA 449C instrument from room temperature to 500°C with a heating rate of 10°C min⁻¹, under nitrogen flow.

2.2. Synthesis

2.2.1. Preparation of [Eu(μ -NAP)₄(NAP)₂(phen)₂] · H₂O (1**).** The solution of 10 mL H₂O dissolved Eu(NO₃)₃ · 6H₂O (0.50 mmol) was added dropwise into an ethanol solution containing phen (0.50 mmol) and the mixed solution was stirred for 0.5 h. Then 15 mL of H₂O solution containing NAP (1.50 mmol) and NaOH (1.50 mmol) was added to the above solution, and the mixed solution was stirred for 4 h. Single crystals were obtained after the filtrate stood at room temperature for 20 days. Yield 88.4% (based on NAP). Anal. Calcd for C₈₄H₈₀N₁₀O₂₀Eu₂ (%): C, 59.29; H, 4.74; and N, 8.23. Found (%): C, 59.25; H, 4.71; and N, 8.20. IR(KBr, cm⁻¹): 3430 m, 2950 w, 1750 s, 1600 s, 1545 w, 1480 m, 1300 s, 1190 w, 1168 w, and 1000 w.

2.2.2. Preparation of [Tb(μ -NAP)₄(NAP)₂(phen)₂] · H₂O (2**).** The preparation method of **2** is similar to that of **1** except that Eu(NO₃)₃ · 6H₂O was replaced by Tb(NO₃)₃ · 6H₂O. The yield of the colorless transparent single crystals is 88.4% (based on NAP). Anal. Calcd for C₈₄H₈₀N₁₀O₂₀Tb₂ (%): C, 59.29; H, 4.74; and N, 8.23. Found (%): C, 59.26; H, 4.72; and N, 8.20. IR(KBr, cm⁻¹): 3450 s, 2970 w, 1745 s, 1580 s, 1540 w, 1485 m, 1295 s, 1175 w, 1160 w, and 1050 w.

2.3. X-ray crystallography

Crystal structure determinations of **1** and **2** were performed on a Bruker Smart APEX II CCD diffractometer with graphite-monochromated Mo-K α radiation ($\lambda = 0.71073 \text{ \AA}$) at 298(2) K. The structure was solved by direct methods and successive Fourier difference synthesis (SHELXS-97) [18] and refined by full-matrix least-squares on F^2 with anisotropic thermal parameters for all non-hydrogen atoms (SHELXL-97) [19]. Corrections for Lp factors were applied. Hydrogens of water were located in the difference Fourier map and other hydrogens were placed in calculated positions; all hydrogens were refined using a riding model in their as-found relative positions. Crystal data and details on refinements for **1** and **2** are summarized in table 1. Selected bond distances and angles are listed in table 2. Hydrogen-bonding data of **1** are listed in table S1.

3. Results and discussion

3.1. Crystal structure

Single-crystal X-ray structural analysis reveals that **1** and **2** are isostructural, and thus only the structure of **1** is described here in detail. As shown in figure 1, each Eu(III) is

Table 1. Crystal data and structure refinement for **1** and **2**.

Compound	1	2
Empirical formula	C ₈₄ H ₈₀ N ₁₀ O ₂₀ Eu ₂	C ₈₄ H ₈₀ N ₁₀ O ₂₀ Tb ₂
Formula weight	1853.50	1867.42
Crystal system	Triclinic	Triclinic
Space group	<i>P</i> $\bar{1}$	<i>P</i> $\bar{1}$
Unit cell dimensions (Å, °)		
<i>a</i>	11.7519(11)	11.779(6)
<i>b</i>	13.4293(12)	13.423(7)
<i>c</i>	14.0686(13)	14.115(7)
α	65.0620(10)	64.968(5)
β	86.1970(10)	86.193(7)
γ	81.8020(10)	81.908(6)
Volume (Å ³), <i>Z</i>	1992.7(3), 1	2001.9(18), 1
Calculated density (g cm ⁻³)	1.545	1.549
Absorption coefficient (mm ⁻¹)	1.639	1.831
θ range for data collection (°)	1.77–25.50	1.59–25.01
Goodness-of-fit on <i>F</i> ²	1.048	1.090
Final <i>R</i> indices [<i>I</i> > 2 σ (<i>I</i>)] ^a	<i>R</i> ₁ = 0.0277, <i>wR</i> ₂ = 0.0663	<i>R</i> ₁ = 0.0389, <i>wR</i> ₂ = 0.0676
<i>R</i> indices (all data)	<i>R</i> ₁ = 0.0299, <i>wR</i> ₂ = 0.0674	<i>R</i> ₁ = 0.0557, <i>wR</i> ₂ = 0.0757

$$^a R = \frac{\sum ||F_o| - |F_c||}{\sum |F_c|} \text{ and } wR_2 = \frac{[\sum [w(F_o^2 - F_c^2)^2]]}{\sum [(F_o^2)^2]}^{1/2}.$$

nine-coordinate with a N₂O₇ donor set by two nitrogens from phen and seven carboxylate oxygens from five NAP ligands. The Eu–O and Eu–N distances range from 2.3929(19) Å to 2.611(2) Å (table 2), similar to those observed in the reported dinuclear Ln compounds [20]. The longest Eu–O distance is associated with one carboxylate oxygen of a coordinated NAP which bridges two Eu centers with Eu...Eu separation of 3.894 Å. Two Eu(III) ions are bridged by four carboxylates, forming the binuclear unit. The binuclear units are arranged in a head-to-tail fashion to facilitate formation of self-complementary double O–H...O hydrogen-bonding interactions between carbonyl oxygens of NAP anions and oxygens of lattice waters (table S1), resulting in a 1-D chain structure along the *c*-axis (figure 2). The two phen ligands of each binuclear unit are extended outward in two different directions and they play a very important role in self-assembly *via* aromatic π – π interactions to form high-dimensional motifs. As shown in figure 3, the binuclear unit, with the terminal phen ligands out from the sides, is arranged in a corner-to-corner fashion (centroid–centroid distances of 3.66 Å), which forms a 2-D layer structure. As a result, the 2-D layers are further assembled into a 3-D supramolecular network and water stabilizes the crystal lattice (figure 4).

Each NAP exhibits three different modes of coordination of carboxylates. One carboxylate is bidentate chelating (κ^2)– μ_1 to coordinate to one Eu(III) (scheme 1b). The other carboxylate is bidentate bridging (κ^1)–(κ^1)– μ_2 to two metals, forming the binuclear unit (scheme 1c). Another carboxylate is bidentate chelating and monodentate bridging (κ^2 – μ_2)– μ_2 mode (scheme 1d). Such diverse coordination modes of carboxylates occurring are relatively scarce.

3.2. Spectroscopic properties

IR spectra were performed as KBr pellets from 4000 to 400 cm⁻¹ (see Supplementary material figures S1 and S2). The IR spectrum of **1** shows strong asymmetric stretches

Table 2. Selected bond lengths (Å) and angles (°) for **1** and **2**.

1			
Eu1–O2	2.611(2)	Eu1–O3#1	2.3929(19)
Eu1–O3	2.4815(19)	Eu1–O7	2.505(2)
Eu1–O4	2.3550(19)	Eu1–O8	2.439(2)
Eu1–O5A	2.3996(19)	Eu1–N4	2.598(2)
Eu1–N5	2.560(2)		
O4–Eu1–O3#1	72.85(7)	O4–Eu1–O5#1	139.06(7)
O3A–Eu1–O5#1	73.33(7)	O4–Eu1–O8	131.38(7)
O3A–Eu1–O8	97.02(7)	O5A–Eu1–O8	75.18(7)
O4–Eu1–O3	76.05(7)	O3–Eu1–O3#1	73.99(7)
O5A–Eu1–O3	72.99(7)	O8–Eu1–O3	148.18(7)
O4–Eu1–O7	78.89(7)	O3A–Eu1–O7	76.54(7)
O5A–Eu1–O7	114.47(7)	O8–Eu1–O7	52.70(7)
O3–Eu1–O7	145.73(6)	O4–Eu1–N5	82.68(7)
O3A–Eu1–N5	142.54(7)	O5A–Eu1–N5	137.86(7)
O8–Eu1–N5	78.16(8)	O3–Eu1–N5	127.34(7)
O7–Eu1–N5	71.13(7)	O4–Eu1–N4	132.05(7)
O3A–Eu1–N4	151.70(7)	O5A–Eu1–N4	78.38(7)
O8–Eu1–N4	76.23(8)	O3–Eu1–N4	97.12(7)
O7–Eu1–N4	117.06(7)	N5–Eu1–N4	63.86(7)
O4–Eu1–O2	72.26(7)	O3A–Eu1–O2	119.70(6)
O5A–Eu1–O2	106.21(7)	O8–Eu1–O2	142.41(7)
O3–Eu1–O2	50.76(6)	O7–Eu1–O2	139.21(7)
N5–Eu1–O2	77.04(7)	N4–Eu1–O2	67.62(7)
2			
Tb1–N4	2.542(4)	Tb1–N5	2.579(4)
Tb1–O1#2	2.373(3)	Tb1–O1	2.464(3)
Tb1–O2	2.608(3)	Tb1–O4	2.422(3)
Tb1–O5	2.497(3)	Tb1–O7	2.337(3)
Tb1–O8A	2.387(3)		
O7–Tb1–O1#2	73.36(10)	O7–Tb1–O8#2	139.77(10)
O1A–Tb1–O8#2	73.34(11)	O7–Tb1–O4	131.38(11)
O1A–Tb1–O4	97.28(11)	O8A–Tb1–O4	74.89(11)
O7–Tb1–O1	76.32(10)	O1–Tb1–O1#2	73.95(11)
O8A–Tb1–O1	73.31(10)	O4–Tb1–O1	148.20(11)
O7–Tb1–O5	78.37(11)	O1A–Tb1–O5	76.27(10)
O8A–Tb1–O5	114.41(11)	O4–Tb1–O5	53.30(11)
O1–Tb1–O5	145.26(10)	O7–Tb1–N4	81.71(11)
O1A–Tb1–N4	142.34(12)	O8A–Tb1–N4	138.14(12)
O4–Tb1–N4	78.40(11)	O1–Tb1–N4	127.07(11)
O5–Tb1–N4	71.31(11)	O7–Tb1–N5	131.91(11)
O1A–Tb1–N5	151.23(12)	O8A–Tb1–N5	77.92(12)
O4–Tb1–N5	76.05(12)	O1–Tb1–N5	96.84(11)
O5–Tb1–N5	117.80(11)	N4–Tb1–N5	64.63(13)
O7–Tb1–O2	71.91(10)	O1A–Tb1–O2	119.99(9)
O8A–Tb1–O2	106.92(11)	O4–Tb1–O2	141.96(11)
O1–Tb1–O2	51.22(9)	O5–Tb1–O2	138.57(11)
N4–Tb1–O2	76.33(11)	N5–Tb1–O2	67.59(11)

Symmetry codes: #1: $-x, -y+2, -z+1$; #2: $-x+1, -y+1, -z+1$.

$\nu_{\text{as}}(\text{COO}^-)$ and symmetric stretches $\nu_{\text{s}}(\text{COO}^-)$ at 1750, 1600 and 1545, 1480 cm^{-1} , respectively, indicating that carboxylates are either coordinated to the metal in a monodentate [21] or bis(chelating bidentate) [22], consistent with the observed X-ray crystal structure of **1**. The solid-state luminescent properties of **1** and **2** were investigated. The emission spectra at excitation wavelength of 380 and 360 nm exhibit characteristic emissions of Eu^{3+} and Tb^{3+} , respectively. The emission spectra

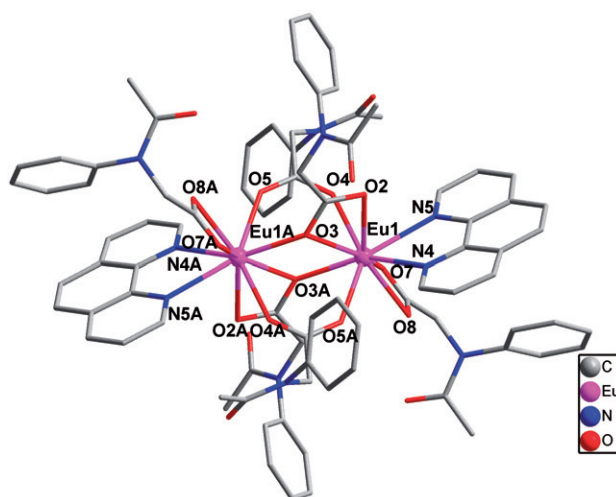


Figure 1. Coordination environment of Eu(III) in **1**. Hydrogens and solvent molecules are omitted for clarity. Symmetry code; #1: $-x, -y+2, -z+1$.

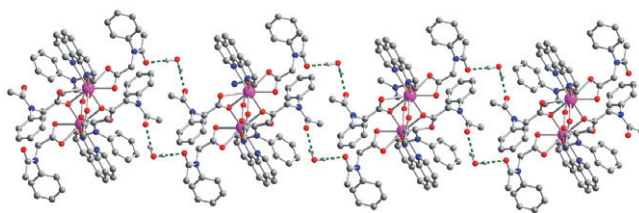


Figure 2. View of the hydrogen bonding 1-D chain in **1** along the c -axis.

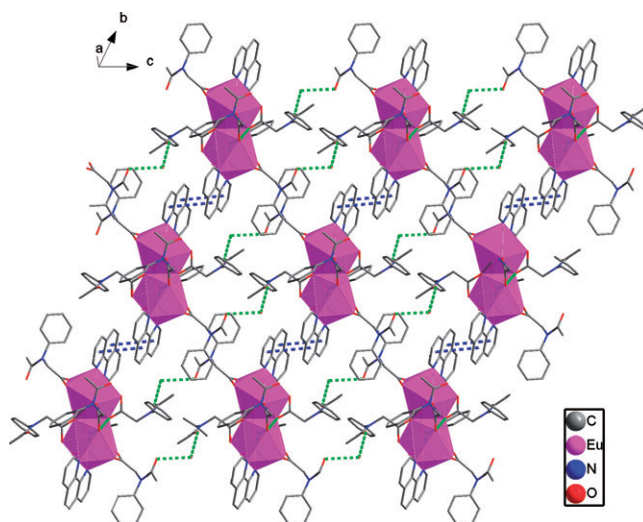


Figure 3. The 2-D layer *via* hydrogen bonding and phen...phen stacking in **1** in the bc plane.

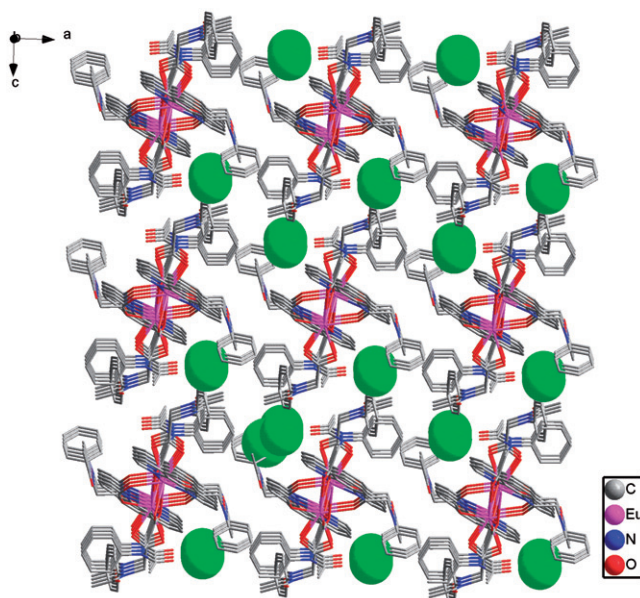


Figure 4. The extended 3-D structure viewed along the *b*-axis.

principally arise from transitions originating at the 5D_0 and 5D_4 levels, respectively. Both complexes show strong fluorescent emission at room temperature. Compound **1** exhibits several characteristic emission bands for f-f transitions of isolated europium(III) ions in the visible region excited at 380 nm (figure 5a). These emission bands are 595 ($^5D_0 \rightarrow ^7F_1$), 620 ($^5D_0 \rightarrow ^7F_4$), and 698 nm ($^5D_0 \rightarrow ^7F_2$). The strongest emission is attributed to the hypersensitive $^5D_0 \rightarrow ^7F_2$ transition at 698 nm, which is typical of Eu(III). Under excitation at 360 nm, **2** displays characteristic emissions for isolated terbium(III) (figure 5b) with four emission bands at 490 ($^5D_4 \rightarrow ^7F_6$), 545 ($^5D_4 \rightarrow ^7F_5$), 583 ($^5D_4 \rightarrow ^7F_4$), and 620 nm ($^5D_4 \rightarrow ^7F_3$); the strongest emission corresponds to $^5D_4 \rightarrow ^7F_5$. The strong emission in fluorescence spectra of the two compounds could be accounted for by the supramolecular interactions in such structures, which suggest that energy transferred from the ligand to the metal centers is quite effective and can sensitize the lanthanide emission.

3.3. Thermogravimetric analysis

Thermal stabilities of **1** and **2** have been investigated by thermogravimetric and differential thermogravimetric (TG-DTG) techniques. Compounds **1** and **2** are isostructural, and the thermogravimetric curve of **1** is discussed here (see Supplementary material figure S3). The TG analysis shows that weight loss of **1** begins at 80°C, with two lattice waters lost from 80°C to 150°C (Calcd 1.9%; found, 1.9%) with derivative weight peaking at 120°C. The second weight loss occurs at 150–250°C, attributed to consecutive removal of phen moieties (Calcd 19.8%; found, 17.1%) with derivative peaking at 225°C. The remaining framework is decomposed through two consecutive weight losses beginning at 250°C and not ending until 500°C. The total

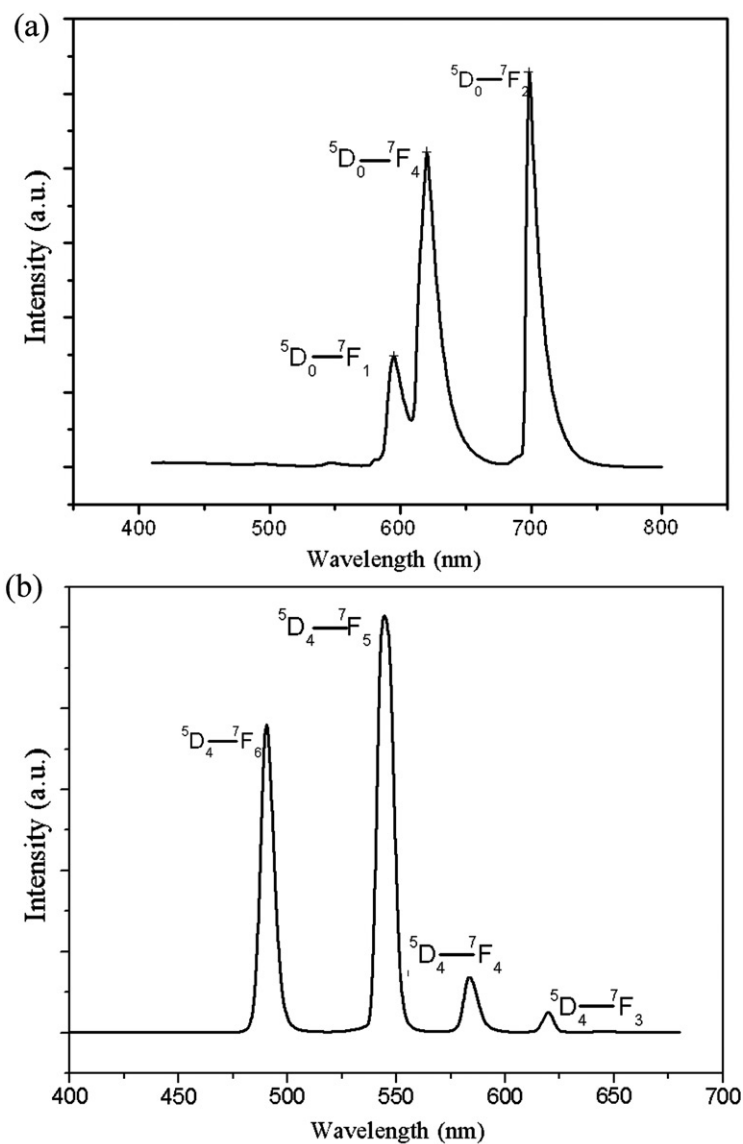


Figure 5. Solid-state emission spectra of (a) **1** and (b) **2** at room temperature upon excitation at 380 and 360 nm, respectively.

weight loss at 500°C is 65.1%, (Calcd 63.5%), and the final residual is expected to be europium(III) oxide.

4. Conclusion

Ln-carboxylate coordination polymers could have structural motifs with various topologies and useful functional properties. Many rare-earth complexes based on

aliphatic polycarboxylate and aromatic acids have been constructed and exhibit interesting properties [23–28]. In this contribution, we chose N-substituent amino acids and isolated two isomorphous binuclear compounds **1** and **2**. The compounds show similar 2-D supramolecular layer structures *via* hydrogen bonding and π – π interactions and display strong characteristic emission of rare-earth coordination polymers. Compared to reported rare-earth complexes based on rigid conjugated aromatic acid ligands [29], the emission intensity of the isomorphous compounds based on NAP is weak, which indicates that the energy transfer from NAP to lanthanide(III) is inefficient in energy transfer. Subsequent work will focus on the structures and photochemical properties of new coordination complexes constructed by conjugated polycarboxylate acid ligands with the special configurations and different metal ions.

Supplementary material

Crystallographic data for the structural analysis have been deposited with the Cambridge Crystallographic Data Centre, CCDC nos 628725 and 628728 for **1** and **2**. Copies of this information may be obtained free of charge on application to CCDC, 12 Union Road, Cambridge CB21EZ, UK (Fax: +44-1223-336033; Email: deposit@ccdc.cam.ac.uk or www: <http://www.ccdc.cam.ac.uk>).

Acknowledgments

The authors gratefully acknowledge the supports from the National Natural Science Foundation of China (no. 20771021) and Shandong Natural Science Foundation (no. Y2005B20).

References

- [1] C. Piguet, J.C.G. Bunzli, G. Bernardinelli, G. Hopfgartner, S. Petoud, O. Schaad. *J. Am. Chem. Soc.*, **118**, 6681 (1996).
- [2] C. Piguet, E.R. Minten, G.J.C. Bernardinelli, G. Bunzli, G. Hopfgartner. *J. Chem. Soc., Dalton Trans.*, 421 (1997).
- [3] F. Renaud, C. Piguet, G. Bernardinelli, J.C.G. Bunzli, G. Hopfgartner. *J. Am. Chem. Soc.*, **121**, 9326 (1999).
- [4] H. Tsukube, S. Shinoda. *Chem. Rev.*, **102**, 2389 (2002).
- [5] A.K. Cheetham, A.K. Cheetham, G. Ferey, T. Loiseau. *Angew. Chem. Int. Ed.*, **38**, 3268 (1999).
- [6] S.R. Batten, R. Robson. *Angew. Chem. Int. Ed.*, **37**, 1460 (1998).
- [7] B. Li, W. Gu, L.Z. Zhang, J. Qu, Z.P. Ma, X. Liu, D.Z. Liao. *Inorg. Chem.*, **45**, 10425 (2006).
- [8] (a) C.D. Gatteschi. *Chem. Rev.*, **102**, 2369 (2002); (b) J. Kido, Y. Okamoto. *Chem. Rev.*, **102**, 2357 (2002); (c) C. Piguet, G. Bernardinelli, G. Hopfgartner. *Chem. Rev.*, **97**, 2005 (1997).
- [9] N. Sabbatini, M. Guardigli, J.M. Lehn. *Coord. Chem. Rev.*, **123**, 201 (1993).
- [10] C. Reinhard, H.U. Gudel. *Inorg. Chem.*, **41**, 1048 (2002).
- [11] H. Zhao, M.J. Bazile, J.R. Galan-Mascaros, K.R. Dunbar. *Angew. Chem. Int. Ed.*, **42**, 2289 (2003).
- [12] (a) G.B. Gardner, D. Venkataraman, J.S. Moore, S. Lee. *Nature*, **374**, 792 (1995); (b) O.R. Evans, W. Lin. *Acc. Chem. Res.*, **35**, 511 (2002); (c) S.L. James. *Chem. Soc. Rev.*, **32**, 276 (2003); (d) D. Bradshaw, T.J. Prior, E.J. Cussen, J.B. Claridge, M.J. Rosseinsky. *J. Am. Chem. Soc.*, **126**,

- 6106 (2004); (e) F.N. Shi, L. Cunha-Silva, R.A. Sa, L. Ferreira, T. Mafra, L.D. Trindade, F.A. Carlos, J. Almeida Paz, J. Rocha. *J. Am. Chem. Soc.*, **130**, 150 (2008).
- [13] (a) S.J. Dalgarno, M.J. Hardie, J.L. Atwood, J.E. Warren, C.L. Raston. *New J. Chem.*, **29**, 649 (2005); (b) A.Y. Robin, K.M. Fromm. *Coord. Chem. Rev.*, **250**, 2127 (2006); (c) O. Guilou, C. Daiguebonne, M. Camara, N. Kerbellec. *Inorg. Chem.*, **45**, 8468 (2006).
- [14] (a) R. Sun, S.N. Wang, H. Xing, J.F. Bai, Y.Z. Li, Y. Pan, X.Z. You. *Inorg. Chem.*, **46**, 8451 (2007); (b) Y. Ouyang, W. Zhang, N. Xu, G.F. Xu, D.Z. Liao, K. Yoshimura, S.P. Yan, P. Cheng. *Inorg. Chem.*, **46**, 8454 (2007); (c) M. Hu, Q.L. Wang, G.F. Xu, B. Zhao, G.R. Deng, Y.H. Zhang, G.M. Yang. *Inorg. Chem. Commun.*, **10**, 1177 (2007).
- [15] (a) B. Zhao, P. Cheng, Y. Dai, C. Cheng, D.Z. Liao, S.P. Yan, Z.H. Jiang, G.L. Wang. *Angew. Chem. Int. Ed.*, **42**, 943 (2003); (b) B. Zhao, P. Cheng, X. Chen, C. Cheng, W. Shi, D.Z. Liao, S.P. Yan, Z.H. Jiang. *J. Am. Chem. Soc.*, **126**, 3012 (2004); (c) C.S. Campos-Fernandez, B.L. Schottel, H.T. Chifotides, J.K. Bera, J. Bacsá, J.M. Koomen, D.H. Russell, K.R. Dunbar. *J. Am. Chem. Soc.*, **127**, 12909 (2005); (d) H.L. Gao, L. Yi, B. Zhao, X.Q. Zhao, P. Cheng, D.Z. Liao, S.P. Yan. *Inorg. Chem.*, **45**, 5980 (2006).
- [16] B. Yan, H.D. Wang, Z.D. Chen. *Polyhedron*, **20**, 591 (2001).
- [17] A.Y. Fu, D.Q. Wang, Q.J. Shen, C.L. Zhang. *Acta Crystallogr. Sect. E*, **60**, m1337 (2004).
- [18] G.M. Sheldrick. *SHELXS 97, Program for Crystal Structure Solution*, University of Göttingen, Göttingen, Germany (1997).
- [19] G.M. Sheldrick. *SHELXL 97, Program for the Refinement of Crystal Structure*, University of Göttingen, Göttingen, Germany (1997).
- [20] (a) X.H. Bu, M. Du, L. Zhang, X.B. Song, R.H. Zhang, T. Clifford. *Inorg. Chim. Acta*, **308**, 143 (2000); (b) X.H. Bu, S.L. Lu, W. Chen, R.H. Zhang. *J. Rare Earths*, **19**, 86 (2001); (c) J.R. Li, R.H. Zhang, X.H. Bu. *Aust. J. Chem.*, **59**, 315 (2006).
- [21] Y.P. Wu, C.J. Wang, Y.Y. Wang, P. Liu, W.P. Wu, Q.Z. Shi, S.M. Peng. *Polyhedron*, **25**, 3533 (2006).
- [22] L. Tang, D.S. Li, F. Fu, J.J. Wang, H.M. Hu, Y.Y. Wang. *Chin. J. Chem.*, **25**, 1641 (2007).
- [23] H. Chen, J. Li, Z.G. Sun, Y.Y. Zhu, J. Zhang, Y. Zhao, N. Zhang, X. Lu, L. Liu. *J. Coord. Chem.*, **62**, 294 (2009).
- [24] F. Chen, W.M. Lu, Y. Zhu, B. Wu, X.M. Zheng. *J. Coord. Chem.*, **62**, 808 (2009).
- [25] L.J. Zhang, F. Jiang, Y.S. Zhou. *J. Coord. Chem.*, **62**, 1476 (2009).
- [26] Y.F. Liu, D.F. Rong, H.T. Xia, D.Q. Wang, L. Chen. *J. Coord. Chem.*, **62**, 1835 (2009).
- [27] M.E. Burin, A.A. Logunov, G.K. Fukin, M.N. Bochkarev. *J. Coord. Chem.*, **62**, 3134 (2009).
- [28] S. Khanjani, A. Morsali. *J. Coord. Chem.*, **62**, 3343 (2009).
- [29] Y.F. Han, X.H. Zhou, Y.X. Zheng, Z. Shen, Y. Song, X.Z. You. *CrystEngComm*, **10**, 1237 (2008).